Since January 2020 Elsevier has created a COVID-19 resource centre with free information in English and Mandarin on the novel coronavirus COVID-19. The COVID-19 resource centre is hosted on Elsevier Connect, the company's public news and information website.

International Journal of Infectious Diseases 95 (2020) 106–112

Contents lists available at ScienceDirect

International Journal of Infectious Diseases

journal homepage: www.elsevier.com/locate/ijid

High-resolution Chest CT Features and Clinical Characteristics of Patients Infected with COVID-19 in Jiangsu, China

Hui Dai[a,b,1], Xin Zhang[c,1], Jianguo Xia[d], Tao Zhang[e], Yalei Shang[a], Renjun Huang[a], Rongrong Liu[f], Dan Wang[g], Min Li[f,2,*], Jinping Wu[g,3,*], Qiuzhen Xu[h,4,*], Yonggang Li[a,b,*]

[a] Department of Radiology, the First Affiliated Hospital of Soochow University, Suzhou city, Jiangsu province, 215000 P.R. China
[b] Institute of Medical Imaging, Soochow University, Suzhou city, Jiangsu province, 215000 P.R. China
[c] Department of Radiology, the Fourth People's Hospital of Huaian, Huai'an city, Jiangsu province, 223001 P.R. China
[d] Department of Radiology, Taizhou People's Hospital, Hospital Affiliated 5 to Nantong University, Taizhou city, Jiangsu province, 225300 P.R. China
[e] Department of Radiology, the Third Hospital Affiliated of Nantong University, Nantong City, Jiangsu province, 226000 P.R. China
[f] Department of Radiology, The Affiliated Infectious Diseases Hospital of Soochow University, Suzhou city, Jiangsu province, 215000 P.R. China
[g] Department of Radiology, the Third People's Hospital of Changzhou, Changzhou city, Jiangsu province, 213000 P.R. China
[h] Department of Radiology, Zhongda Hospital Affiliated to Southeast University, Nanjing city, Jiangsu province, 210000 P.R. China

ARTICLE INFO

Article history:
Received 26 February 2020
Received in revised form 30 March 2020
Accepted 1 April 2020

Keywords:
SARS-CoV-2
COVID-19
High-resolution CT (HRCT)

ABSTRACT

Background: A pneumonia associated with the coronavirus disease 2019 (COVID-19) recently emerged in China. It was recognized as a global health hazard.
Methods: 234 inpatients with COVID-19 were included. Detailed clinical data, chest HRCT basic performances and certain signs were recorded Ground-glass opacity (GGO), consolidation, fibrosis and air trapping were quantified. Both clinical types and CT stages were evaluated.
Results: Most patients (approximately 90%) were classified as common type and with epidemiologic history. Fever and cough were main symptoms. Chest CT showed abnormal attenuation in bilateral multiple lung lobes, distributed in the lower and/or periphery of the lungs (94.98%), with multiple shapes. GGO and vascular enhancement sign were most frequent seen, followed by interlobular septal thickening and air bronchus sign as well as consolidation, fibrosis and air trapping. There were significant differences in most of CT signs between different stage groups. The SpO2 and OI were decreased in stage IV, and the CT score of consolidation, fibrosis and air trapping was significantly lower in stage I ($P < 0.05$). A weak relevance was between the fibrosis score and the value of PaO2 and SpO2 ($P < 0.05$).
Conclusions: Clinical performances of patients with COVID-19, mostly with epidemiologic history and typical symptoms, were critical valuable in the diagnosis of the COVID-19. While chest HRCT provided the distribution, shape, attenuation and extent of lung lesions, as well as some typical CT signs of COVID-19 pneumonia.

1. Introduction

In December 2019, an outbreak of pneumonia of unknown etiology was reported in Wuhan, Hubei province, China. The Chinese Center for Disease Control and Prevention (CDC) isolated the causative viral pathogen from throat swabs sample of the affected patients. The pathogen was a novel coronavirus named severe acute respiratory syndrome coronavirus 2 (SARS-CoV-2) by WHO and the disease caused by SARS-CoV-2 was termed as coronavirus disease 2019 (COVID-19). Up to February 18, 2020, 58097 laboratory-confirmed cases of COVID-19 and 1870 deaths have been reported in China, posing great threats to global public health.

* Corresponding author at: Department of Radiology, the First Affiliated Hospital of Soochow University, Suzhou, Jiangsu, 215000 P.R. China. Tel.: +0086 512 67780155; fax: +0086 512 65228072.
E-mail addresses: 105549156@qq.com (M. Li), czwjp@sina.com (J. Wu), xuqiuzhen831@sina.com (Q. Xu), liyonggang224@163.com (Y. Li).
[1] These authors contributed equally to this work.
[2] Department of Radiology, The Affiliated Infectious Diseases Hospital of Soochow University, Suzhou city, Jiangsu province, P.R. China 215000, Tel.: 0086 512 67780633; fax: 0086 512 67780633
[3] Department of Radiology, the Third People Hospital of Changzhou, Changzhou city, Jiangsu province, P.R.China 213000, Tel.: 0086 519 82009212; fax: 0086 519 82009212
[4] Department of Radiology, Zhongda Hospital Affiliated to Southeast University, Nanjing city, Jiangsu province, P.R. China 210000

https://doi.org/10.1016/j.ijid.2020.04.003

SARS-CoV-2, severe acute respiratory syndrome coronavirus (SARS-CoV) and the Middle East respiratory syndrome coronavirus (MERS-CoV) (Ksiazek et al., 2003; K Kuiken et al., 2003; de Groot et al., 2013) are subgroups of betacoronavirus genus. As far as we known, the symptoms of COVID-19 range from mild to severe. They can be fever, dry cough, shortness of breath, and in some severe cases, kidney failure or death similar to SARS-CoV infection may occur (Huang et al., 2020). However, information regarding to the radiological and clinical features of the pneumonia associated with COVID-19 is still scarce, making it difficult for physicians to distinguish the causative agents without genetic related laboratory analysis. Moreover, reverse transcription-polymerase chain reaction (RT-PCR), the gold standard for a confirmative diagnosis of COVID-19, has some limitations, such as certain proportion of false negative results, limited sampling method and shortage of kits. Computed tomography (CT) of the chest is increasingly recognized as strong evidence for early diagnosis, because the changes in chest imaging sometimes maybe earlier than clinical symptoms. Considering that fewer confirmed cases were included in previous studies (Chung et al., 2020), we set up a Jiangsu multi-center study, to collect a considerable larger sample size in this retrospective study. The purpose of the study is to improve the comprehension of the newly-emerged diseases in order to make the diagnosis earlier, by describing the comprehensive chest CT characteristics and clinical features of patients with COVID-19, who were admitted to the designated hospitals in Jiangsu province, China.

2. Methods

2.1. Patients and clinical data

This study was conducted in accordance with the amended Declaration of Helsinki. Independent ethics committees approved the protocol, and written informed consent was obtained from all patients. This was a multi-centered study included 234 inpatients from 13 hospitals during 17 days (from January 10th to February 7th 2020) in Jiangsu. All the cases were confirmed with the criteria for SARS-CoV-2 infection established by National Health Commission, which was consistent with one of the following two conditions, based on the pathogenic evidence: 1) positive in real-time fluorescent RT-PCR detection of novel coronavirus nucleic acid in specimens from respiratory tract or blood; 2) virus was highly homologous to the known novel coronavirus in genetic sequencing analyses in specimens from respiratory tract or blood. All the cases underwent an additional microbiological evaluation for ruling out other suspected respiratory infections. Those with a proved additional concurrent acute illness or other preexisting medical conditions were also excluded.

Clinical data were recorded, containing age, gender, occupation, epidemic history and disease severity. Present history, symptoms and signs, blood routine outcomes and therapeutic schedules were also recorded. There were four clinical types according to the severity of disease – mild type, subtle or mild clinical symptoms and no pneumonia found on CT images; common type, fever or respiratory symptoms, etc. and pneumonia observed on CT images; severe type, fulfil any one of the following conditions 1) respiratory distress, respiratory rate (RR) $\geq$30 times per minute, 2) resting state oxygen saturation (SpO2) $\leq$93%, or 3) oxygenation index (OI) (calculated by partial pressure of oxygen (PaO2)/fraction of inspired oxygen (FiO2)) $\leq$300 mmHg (1 mmHg = 0.133 kPa); critical severe type, fulfil any one of the following conditions 1) respiratory failure and mechanical ventilation needed, 2) shock, 3) combined failure of other organ and ICU monitoring and treatment needed.

2.2. CT scanning

Each subject underwent chest high-resolution CT (HRCT) examination within 24 hours after admission. Inspiratory phase of chest HRCT examination was performed during a single-breath hold at full inspiration. The CT scanner models from the hospitals involved in this multicenter study were listed as following: GE Bright Speed Elite 16, Neusoft 16, SOMATOM Emotion, SOMATOM definition AS, PHLIPS MX-16, Philips 64-row spiral Ingenuity and the UNITED IMAGING Elite 16. The scanning parameters were as following: tube voltage 120 kV, tube current 110 mA, pitch 1.0, rotation time ranging from 0.5s to 0.75s, slice thickness 5 mm, with 1 mm or 1.5 mm section thickness for axial, coronal and sagittal reconstructions.

2.3. CT evaluation

Two experienced attending radiologists, blinded to the clinical information, separately reviewed and scored the CT images. The expert group, containing 3 senior radiologists with working experience more than 10 years, would make the final decision if there was a divergent opinion between the two attending.

1. Basic CT performances
   The distribution features and the shape of abnormal attenuation, as well as the involved lung lobes, were recorded. If there were any common accompanying diseases of lung, such as obsolete pulmonary tuberculosis, emphysema, bronchiectasia, tumor and others, they would be recorded.
2. Certain CT signs
   The following CT performances were judged and recorded as 0 or 1 (0 for none, 1 for yes), including vascular enhancement sign (VES, vascular enlargement inside the lesion resulted from congestion and dilation of small vessels), air bronchus sign, reticular/mosaic sign (defined as a collection of innumerable small linear opacities that, by summation, produced an appearance resembling a net (Yun et al., 2011)), bronchial wall thickening, interlobular septal thickening, interlobar fissure displacement, solid nodules, intralesional and/or perilesional bronchiectasis, mediastinal lymphadenopathy, pleural effusion, pleural thickening and pericardial effusion.
3. Quantified evaluation
   The signs of ground-glass opacity (GGO), consolidation, fibrosis and air trapping were analyzed quantitatively using a radiologic scoring system ranging from 0-25 points, which was an adaptation of the method previously used to describe idiopathic pulmonary fibrosis and SARS (Ng et al., 2004). Each lung lobe was evaluated by 0-5 points, on the basis of the area involved, with score 0 for normal performance, 1 for less than 5% of lung lobe areas involved, 2 for 6%–25%, 3 for 26%–50%, 4 for 51%–75%, and 5 for more than 75%. A total score was eventually recorded via the addition of the score of each lobe.
4. CT stages
   According to the performances of CT images, the cases were classified into four stages–stage I (early stage), stage II (progressive stage), stage III (recovery stage), and stage IV (severe stage). The classification method was mainly according to the following CT performances. Stage I: single or multiple lesions, in irregular, round-like or patchy shapes, generally not involved the whole lung segment, often showed GGO with vascular enlargement. Stage II: more extensive lesions, involved bilateral multiple lobes predominantly in the subpleural areas, in irregular, round-like, patchy and “anti-butterfly” shapes, scattered or diffused patches even fusing into large patches with density increased, often with vascular enlargement, reticular sign and bronchial wall thickening,

occasionally with less fibrosis and sub-segment atelectasis. Stage III: the lesions absorbed and diminished, the focus can be completely absorbed, with residual fiber stripes. Stage IV: bilateral diffuse lesions, more than half of the lung field involved, even extended to the whole lung and presented as "white lung".

2.4. Statistical analysis

The statistical analyses were performed by Statistical Product and Service Software (SPSS ver. 26.0, Chicago, IL, USA). Descriptive statistics was used in clinical data and some basic information of CT images. Pearson Chi-square test and Fisher exact probability test were used in dichotomous variables (0 or 1) to test the differences of these variables among different CT stages groups. Kruskal–Wallis H test was used to test the group differences of multiple quantitative variables (arterial blood gas (ABG) analysis results and CT scoring). Spearman rank correlation was used to measure the degree of association between the ABGanalysis results and CT scoring. A P value less than 0.05 was considered statistically significant and Bonferroni correction was used to adjust P values in multiple comparisons. The mean values were showed as MEAN $\pm$ SE.

3. Results

3.1. Clinical data

234 patients infected with SARS-CoV-2 confirmed by real time RT-PCR were included in this study, among which 6 patients were with initial RT-PCR negative and follow-up test positive. There were 136 (58.1%) men and 98 (41.9%) women, with average age (44.6 ± 14.8) years old (ranging from 7 to 82 years old). The age and occupation distribution of the patients were showed in Table 1. Stuff was the most frequency occupation (46.2%) in this study. Approximately 90% patients had epidemiologic linkage to Hubei Province or closely contacted with other confirmed cases and almost 90% patients were classified as common type, as showed in Table 1.

Fever (72.6%) and cough (64.1%) were main symptoms of patients infected with SARS-CoV-2. There were some other symptoms such as pharyngeal discomfort (15%), fatigue (13.2%), chill (9.8%), muscle ache (9.0%), rhinobyon and snivel (5.6%), diarrhea (3.8%), chest pain (3.4%), chest tightness (5.6%), short of breath (2.1%), difficulty breathing (3%) and nausea and vomiting (2.1%). Most of patients were with normal range of leukocytes count, neutrophils count, lymphocytes count, neutrophil ratio and lymphocyte ratio in the first blood routine examination during hospitalization. The proportion of normal cases were respectively 75.1%, 81.7%, 59.7%, 82.6% and 59.7% of all the patients. As to the therapy schedules, each patient was received an antiviral therapy (oral or intravenous antiviral drugs, and inhalation of interferon). Antibiotics was administered in 118 (50.4%) patients to prevent or treat concomitant bacterial infection, methylprednisolone in 34 (14.5%) to suppress the inflammatory response, gamma globulin in 34 (14.5%) to boost immunity, and non-invasive ventilator was used in 11 (4.7%) cases (severe or critical severe patients).

3.2. Chest CT analysis

1. Basic CT performances and CT stages

   15 (6.4%) patients were without abnormal lung changes by Chest HRCT examination, hence the CT images of 219 patients were analyzed. 192 cases were with bilateral multiple lung lobes involved (87.67%, 192/219), of which 121 cases (63.02%, 121/192) were involved with whole lung. Merely 16 cases (7.31%, 16/219) were involved with single lobe. 208 cases (94.98%, 208/219) were mainly distributed in the lower lungs and/or the periphery of the lungs. The shape of the lesions was mainly irregular (88.13%, 193/219), followed by small patches (86.3%, 189/219), strip-like (69.41%, 152/219), round-like (49.32%, 108/219) and "anti-butterfly" (47.95%, 105/219). 60 patients (27.4%, 60/219) were with common accompanying diseases of lung, of which emphysema (including localized emphysema) and bullae was the most common (88.33%, 53/60), followed by bronchiectasia (16.67%, 10/60).

   According to the performance of chest CT, the patients were divided into stage I-IV, as the cases showed in Figs. 1–4. 80 cases (36.53%, 80/219) were classified into stage I group, 86 cases

Table 1
Demographics of 234 patients infected with SARS-CoV-2 in Jiangsu, China

Items	Sub-items	Case distribution (number and percentage)
Age (years)	0-9	1(0.4%)
	10-19	4(1.7%)
	20-29	38(16.2%)
	30-39	52(22.2%)
	40-49	47(20.1%)
	50-59	54(23.1%)
	60-69	30(12.8%)
	70-79	7(3.0%)
	80-89	1(0.4%)
Gender	Men	136(58.1%)
	Woman	98(41.9%)
Occupation	None	26(11.1%)
	Stuff	108(46.2%)
	Student	11(4.7%)
	Medical staff	3(1.3%)
	Farmer	26(11.1%)
	Others	60(25.6%)
Epidemic history	epidemiologic linkage to Hubei Province	133(56.8%)
	epidemiologic linkage to other confirmed cases, without traveling to Hubei	78(33.3%)
	None	23(9.8%)
Disease severity	Mild	9 (3.9%)
	Common	210 (89.7%)
	Severe	13(5.5%)
	Critical severe	2(0.9%)

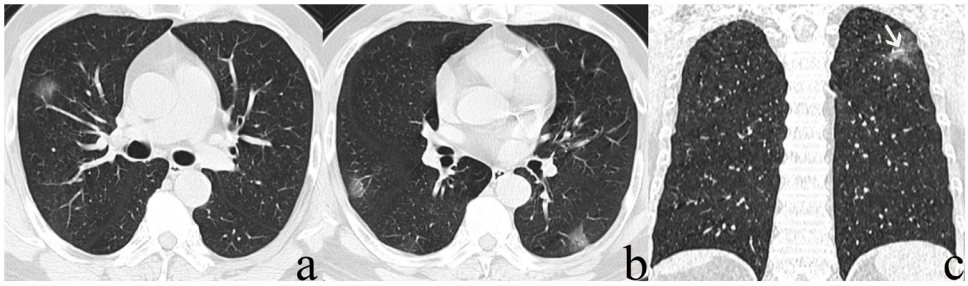

Fig. 1. a–c. A 53-year-old man with COVID-19 in stage I. Chest axial HRCT images a and b show irregular and round-like GGO in bilateral multiple lobes. Coronal reconstruction image c shows VES in the irregular lesion of left upper lung (arrow).

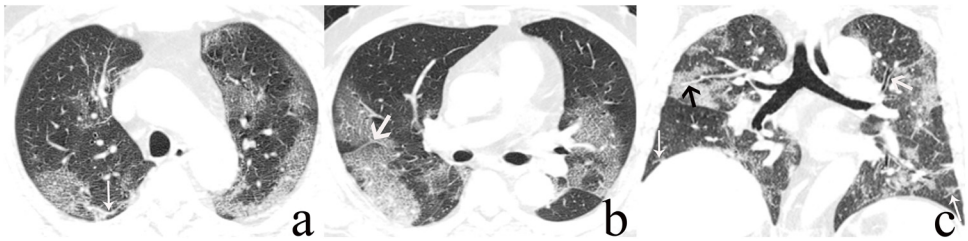

Fig. 2. a-c. A 56-year-old man with COVID-19 in stage II. Chest HRCT images a-c show multiple "anti-butterfly" -shaped and irregular GGO with reticular sign in bilateral lungs. Axial CT image b shows the displacement of right interlobar fissure (arrow). Bronchial wall thickening in left upper lung (white arrow) and VES (black arrow) in middle lobe of right lung can be seen on coronal reconstruction CT image c. A few fibrosis (linear arrow) can be seen in bilateral lungs on image a and c.

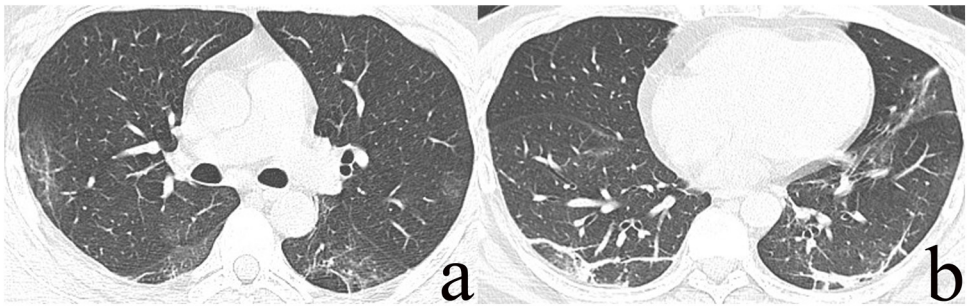

Fig. 3. a, b. A 43-year-old man with COVID-19 in stage III. Chest HRCT images show that the lesions absorbed with multiple residual fiber stripes in both lungs, mainly in the lower lung lobes.

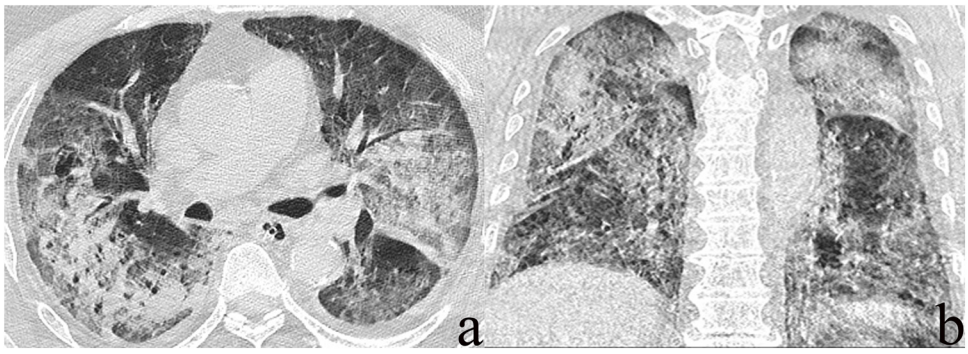

Fig. 4. a, b. A 73-year-old man with COVID-19 in stage IV. Chest HRCT images show bilateral diffuse pneumonia with air bronchus sign.

(39.27%, 86/219) into stage II group, 43 cases (24.2%, 43/219) into stage III group and 10 cases (4.57%, 10/219) into stage IV.

2. Certain CT signs

Among the 219 patients with positive chest HRCT performances, 207 cases were with VES, 205 with interlobular septal thickening, 184 with air bronchus sign, 173 with intralesional and/or perilesional bronchiectasis, 170 with pleural thickening, 138 with solid nodules, 135 with reticular/mosaic sign, 124 with interlobar fissure displacement, 76 with bronchial wall thickening, 29 with minor pleural effusion and pericardial effusion, 21 with mediastinal lymphadenopathy.

The frequency of VES was the highest, but there was no significant difference among the four stage groups, as showed in Table 2. The frequency of interlobular septal thickening, air bronchus sign and intralesional and/or perilesional bronchiectasis in stage I was significantly lower than that in stage II and

Table 2
Comparison of the frequency of HRCT signs among different CT stages

	I-II		I-III		I-IV		II-III		II-IV		III-IV	
	P	χ2	P	χ2	P	χ2	P	χ2	P	χ2	P	χ2
VES	0.051	4.312	0.303	1.071	0.298	1.098	0.474	0.516	0.628	0.238	0.491	0.483
Air bronchus sign	0.000	36.033	0.001	11.118	0.018	5.625	0.025	5.098	0.733	0.118	0.320	1.006
Reticular sign	0.000	33.007	0.001	11.837	0.000	15.395	0.151	2.078	0.110	2.576	0.037	4.425
BWT	0.273	1.209	0.001	10.999	0.002	9.256	0.016	5.895	0.016	5.837	0.347	0.900
IST	0.000	16.436	0.004	8.492	0.152	2.072	–	–	–	–	–	–
IFD	0.000	48.945	0.000	32.987	0.000	26.250	0.886	0.021	0.079	3.126	0.075	3.228
Solid nodules	0.136	2.238	0.036	4.450	0.004	8.221	0.357	0.855	0.022	5.324	0.060	3.607
Bronchiectasis*	0.000	25.624	0.000	20.328	0.041	4.219	0.354	0.867	0.943	0.005	0.514	0.435
Pleural thickening	0.000	26.495	0.000	19.657	0.005	7.854	0.522	0.413	0.285	1.155	0.394	0.740
MI	0.040	4.250	0.002	9.712	0.012	6.410	0.199	1.660	0.373	0.803	0.920	0.010
Pleural effusion	0.014	6.081	0.000	15.763	0.000	27.960	0.070	3.315	0.003	8.930	0.133	2.295
Pericardial effusion	0.682	0.169	0.564	0.335	0.140	2.203	0.347	0.892	0.079	3.126	0.322	0.998

Note: VES- Vascular enhancement sign, Bronchiectasis*- intralesional and/or perilesional bronchiectasis, BWS-Bronchial wall thickening, IST-Interlobular septal thickening, IFD- Interlobar fissure displacement, MI- Mediastinal lymphadenopathy;
"–" in the row of IST without exact number is due to that IST variable was considered as a constant for the identical component ratio of stage II, III and IV.

Table 3
The group differences of SpO2, OI, and CT scores of consolidation, fibrosis and air trapping

	I-II		I-III		I-IV		II-III		II-IV		III-IV	
	P	Z	P	Z	P	Z	P	Z	P	Z	P	Z
SpO2	0.846	−1.472	1.000	0.071	0.083	2.463	0.806	1.497	0.008	3.200	0.096	2.408
OI	0.414	1.818	0.963	1.404	0.009	3.176	1.000	−0.067	0.229	2.073	0.453	1.778
Consolidation	0.001	−3.820	0.009	−3.165	0.191	−2.147	1.000	−0.027	1.000	−0.379	1.000	−0.346
Fibrosis	0.021	−2.917	0.000	−4.520	0.470	−1.760	0.189	−2.150	1.000	−0.411	1.000	0.752
Air trapping	1.000	−0.737	0.544	−1.692	0.045	−2.675	1.000	−1.100	0.115	−2.343	0.601	−1.644

Note: SpO2, oxygen saturation; OI, oxygenation index

Table 4
The correlations between ABG analysis indices and CT scores

	GGO		Consolidation		Fibrosis		Air trapping	
	P	r	P	r	P	r	P	r
RR	0.948	0.006	0.229	0.103	0.842	−0.017	0.896	0.011
PaO2	0.459	0.068	0.202	0.118	0.017	0.218	0.118	0.144
SpO2	0.752	0.031	0.089	0.164	0.032	0.206	0.115	0.235
OI	0.167	0.217	0.740	−0.053	0.571	0.090	0.989	−0.002

Note: ABG, arterial blood gas; GGO, ground-glass opacity; RR, respiratory rate; PaO2, partial pressure of oxygen; SpO2, oxygen saturation; OI, oxygenation index

stage III ($P<0.008$). The frequency of reticular sign, pleural thickening and interlobar fissure displacement was the lowest in stage I ($P<0.008$). The frequency of solid nodules in stage IV was significantly higher than that in stage 1 ($P<0.008$). The frequency of bronchial wall thickening was lower in stage I than that in stage III and stage IV ($P<0.008$).

The frequency of pleural effusion, pericardial effusion and mediastinal lymphadenopathy was relatively small. The frequency of pleural effusion was lower in stage I than that in stage III and stage IV, and it was also lower in stage II than that in stage IV ($P<0.008$). The frequency of mediastinal lymphadenopathy was lower in stage I than that in stage III ($P<0.008$). There was no significant difference of the frequency of pericardial effusion among the four groups.

3.3. Analysis about clinical and CT quantified data

1. Multiple comparisons among stage I-IV groups
   As to the group differences of indices from ABG analysis, the SpO2 ($(94.70\pm0.20)\%$) of patients in stage IV group was significantly lower than that ($(97.2\pm0.91)\%$) in stage II group, and the OI ((200.25 ± 24.75) mmHg) of patients in stage IV was lower than that ((470.71 ± 38.81) mmHg) in stage I ($P<0.05$) (Table 3). There were no significant differences of RR and PaO2 among stage I-IV groups ($P>0.05$).
   As to the group differences of CT scores, the CT score of consolidation (5.71 ± 0.42) in stage I was significantly lower than those in other three groups (respectively 7.06 ± 0.49, 7.60 ± 0.66, 8.30 ± 1.72), and the CT score of fibrosis (1.98 ± 0.24) in stage I was significantly lower than those in stage II (3.00 ± 0.26) and III (4.12 ± 0.41) ($P<0.05$). The air trapping score (0.35 ± 0.10) of inspiratory phase of chest CT was lower in stage I than that in stage IV (1.5 ± 0.76) ($P<0.05$) (Table 3). The GGO score was higher than consolidation, fibrosis and air trapping scores of all the patients, however, there was no significant difference of GGO score among CT stages ($P>0.05$).
2. Correlation analysis
   There were significant correlations among the ABG analysis indices - PaO2, SpO2 and OI, as well as among the CT scores of GGO, consolidation, fibrosis and air trapping. However, there were no correlations between the ABG analysis indices and CT scores ($P>0.05$), except the weak relevance between the fibrosis score and PaO2 ($P=0.017$, $r=0.218$) and between fibrosis score and SpO2 ($P=0.032$, $r=0.206$), as showed in Table 4.

4. Discussion

The SARS-CoV-2 infection is recognized as a global health hazard. The disease is highly infectious. It is suspected that infection is transmitted by means of large-particle respiratory droplets produced by coughing or touch contamination. Hence, good respiratory and hand hygiene is important (Swerdlow, 2020).

A greater number of men (58.1%, 136/234) was found than that of women (41.9%, 98/234), which was similar to previous studies (Chen et al., 2020). The reduced susceptibility of females to viral

infections might be attributed to the protection from X chromosome and sex hormones, which play an important role in innate and adaptive immunity (Jaillon et al., 2019). Almost 90% patients in present study were classified as common type. Fever and cough were main symptoms. However, some patients presented initially with atypical symptoms, such as diarrhea, nausea and vomiting. A large proportion of patients were with normal blood routine examination. Up to February 18, 2020, a total of 629 COVID-19 confirmed cases had been reported without death in Jiangsu Province, compared to Hubei Province 59989 cases with 1789 death. Most cases in Jiangsu were with mild clinical symptoms and approximately 90% patients had epidemiologic linkage to Hubei Province or closely contacted with other confirmed cases in present study, suggesting that the virus might mutate to produce the first generation, the second generation and so on, with the longer the mutation time, the lower the toxicity, as the MERS-CoV (Poletto and Colizza, 2016; Drosten et al., 2014). Because of the relatively lower toxicity, clinical symptoms are slight and the prognosis is relatively good.

As SARS-CoV-2 is highly contagious and with a high incidence, early detection is of great importance. Chest HRCT is a critical screening method for COVID-19 due to its high sensitivity and convenience, although 15 patients with COVID-19 were without abnormal lung changes on initial CT images in present study. Additionally, 6 patients were with pneumonia detected by HRCT, but initial RT-PCR was negative with follow-up test positive. These results suggested that both chest HRCT examination and RT-PCR detection of novel coronavirus nucleic acid had limitations which inevitably lead to false-negative. In the follow-up of the initial negative CT cases, pneumonia would be emerged in some patients, while the initial negative RT-PCR cases would be emerged with positive outcomes after redetection for one time or more than once. It suggestedthe critical importance to combine the two methods in the early stage of the disease to exclude the SARS-CoV-2 infection.

There were some typical findings on CT images. The abnormal attenuations were highly frequently located in bilateral multiple lung lobes and distributed in the lower and/or periphery of the lungs, with the shape of irregular, small patches, strip-like, round-like and “anti-butterfly”. VES was the most frequent sign, followed by interlobular septal thickening, air bronchus sign, intralesional and/or perilesional bronchiectasis, pleural thickening, solid nodules, reticular/mosaic sign, etc. These CT performances of COVID-19 were similar to previous studies (Chung et al., 2020; Noval Coronavirus, 2020). In addition, a few cases of mediastinal lymph node enlargement, pleural effusion and pericardial effusion were found in present study, which were not reported yet. It might be due to the relatively small sample size of previous study. Furthermore, there were group differences of some CT signs among different CT stages, though GGOs and VES sign were most frequently seen in each CT stages without group differences in patients with COVID-19 pneumonia. In the early stage, interlobular septal thickening, air bronchus sign, intralesional and/or perilesional bronchiectasis and bronchial wall thickening were less seen than that in progressive stage. The reticular sign, pleural thickening and interlobar fissure displacement were not common in early stage. The frequency of pleural effusion, pericardial effusion and mediastinal lymphadenopathy was relatively small. The quantified evaluation of CT images demonstrated that consolidation, fibrosis and air trapping were minor in the early stage. These results suggested that each CT stage had its characteristic CT signs and performances, making it possible to radiologists and physicians to quickly obtained the stage of the pneumonia.

As to the ABG results, the SpO2 and OI decreased in patients with severe stage than early or progressed stage, which were in consistence with the alteration of indices in patients with severe or critical severe clinical type. In the severe stage of CT, the bilateral diffuse parenchymal abnormalities were mainly GGO lesions, with consolidation, fibrosis and air trapping. It might demonstrate the severity of pulmonary dysfunction caused by SARS-CoV-2 infection. While the fibrosis score was higher in the recovery stage, which might indicate an improvement of the disease. And a weak positive relevance was found between the fibrosis score and ABG indices (PaO2 and SpO2), that was, a patient with higher fibrosis score tended to have better ABG results, suggesting that fibrosis score might be a potential index in the prognosis of the disease.

There were several limitations in this study. First, the patients underwent the CT scans with different machine type, due to the multiple centers in the study. The heterogeneity of the CT data might affect the results of the study. Second, none of the patients underwent a lung biopsy or autopsy, because of the comparatively better outcomes of the patients in this study. Therefore, the CT findings of the lung could not be verified by histopathology. Finally, this was a retrospective study with initial CT images during hospitalization, mainly demonstrated the early pulmonary lesions in patients with COVID-19. A further longitudinal research was needed to focus on the long-term follow-up, to provide dynamic CT evaluation for pulmonary lesions and to obtain the data of long-term pulmonary function changes.

In conclusion, clinical performances of patients with COVID-19, mostly with epidemiologic history and typical symptoms, were critical valuable in the diagnosis of the COVID-19. While chest HRCT provided the distribution, shape, attenuation and extent of lung lesions, as well as some typical CT signs of COVID-19 pneumonia.

Ethical Approval

Independent ethics committees approved the protocol, and the approval number was respectively 2020 the 30th, 2020001, 2020 the 2th, KY 202000701, E2020002, 2020ZDSYLL016-P01, 02A-A2020002, 202002, 2020 the 6th, 20200217, 2020-SL-0004.

Conflict of interest

No conflict of interest exits in the submission of this manuscript.

Acknowledgments

This work was mainly supported by the National Natural Science Foundation of China (grant number 81971573, 81671743), the Clinical Key diseases diagnosis and therapy Special project of Health and Family Planning Commission of Suzhou (LCZX201801), the Project of Invigorating Health Care through Science, Technology and Education, Jiangsu Provincial Medical Youth Talent (QNRC2016709), the High-level Health Personnel “six-one” Project of Jiangsu Province (LGY2016035) and Program for Advanced Talents within Six Industries of Jiangsu Province (WSW-057).

References

Ksiazek TG, Erdman D, Goldsmith CS, Zaki SR, Peret T, Emery S, Tong S, Urbani C, Comer JA, Lim W, Rollin PE, Dowell SF, Ling AE, Humphrey CD, Shieh WJ, Guarner J, Paddock CD, Rota P, Fields B, DeRisi J, Yang JY, Cox N, Hughes JM, LeDuc JW, Bellini WJ, Anderson LJ, SARS Working Group. A novel coronavirus associated with severe acute respiratory syndrome. N Engl J Med 2003;348:1953–66.

K Kuiken T, Fouchier RA, Schutten M, Rimmelzwaan GF, van Amerongen G, van Riel D, Laman JD, de Jong T, van Doornum G, Lim W, Ling AE, Chan PK, Tam JS, Zambon MC, Gopal R, Drosten C, van der Werf S, Escriou N, Manuguerra JC, Stöhr K, Peiris JS, Osterhaus AD. Lancet 2003;362:263–70.

de Groot RJ, Baker SC, Baric RS, Brown CS, Drosten C, Enjuanes L, Fouchier RA, Galiano M, Gorbalenya AE, Memish ZA, Perlman S, Poon LL, Snijder EJ, Stephens GM, Woo PC, Zaki AM, Zambon M, Ziebuhr J. Middle East respiratory syndrome

coronavirus (MERS-CoV): announcement of the Coronavirus Study Group. J Virol 2013;87:7790–2.
Huang C, Wang Y, Li X, Ren L, Zhao J, Hu Y, Zhang L, Fan G, Xu J, Gu X, Cheng Z, Yu T, Xia J, Wei Y, Wu W, Xie X, Yin W, Li H, Liu M, Xiao Y, Gao H, Guo L, Xie J, Wang G, Jiang R, Gao Z, Jin Q, Wang J, Cao B. Clinical features of patients infected with 2019 novel coronavirus in Wuhan. China.Lancet 2020;395:497–506.
Chung M, Bernheim A, Mei X, Zhang N, Huang M, Zeng X, Cui J, Xu W, Yang Y, Fayad ZA, Jacobi A, Li K, Li S, Shan H. CT Imaging Features of 2019 Novel Coronavirus (COVID-19). Radiology. 2020;200230 [Preprint]. Available from: https://doi.org/10.1148/radiol.2020200230.
Yun TJ, Park CM, Kwon GJ, Woo SK, Park SH, Choi SH, Lee HJ, Goo JM. Clinical and radiological features of pandemic H1N1 2009 influenza virus infection manifesting as acute febrile respiratory illness at their initial presentations: comparison with contemporaneous non-H1N1 patients. Acta Radiol 2011;52:410–6.
Ng CK, Chan JW, Kwan TL, To TS, Chan YH, Ng FY, Mok TY. Six month radiological and physiological outcomes in severe acute respiratory syndrome (SARS) survivors. Thorax 2004;59:889–91.
Swerdlow DL. Preparation for Possible Sustained Transmission of 2019 Novel Coronavirus: Lessons From Previous Epidemics. JAMA 2020; [Preprint]. Available from: https://doi.org/10.1001/jama.2020.1960.
Chen N, Zhou M, Dong X, Qu J, Gong F, Han Y, Qiu Y, Wang J, Liu Y, Wei Y, Xia J, Yu T, Zhang X, Zhang L. Epidemiological and clinical characteristics of 99 cases of 2019 novel coronavirus pneumonia in Wuhan, China: a descriptive study. Lancet 2020;395:507–13.
Jaillon S, Berthenet K, Garlanda C. Sexual dimorphism in innate immunity. Clin Rev Allergy Immunol 2019;56:308–21.
Poletto C, Colizza V. Quantifying spatiotemporal heterogeneity of MERS-CoV transmission in the Middle East region: A combined modelling approach. Epidemics. 2016;15:1–9.
Drosten C, Meyer B, Müller MA, Corman VM, Al-Masri M, Hossain R, Madani H, Sieberg A, Bosch BJ, Lattwein E, Alhakeem RF, Assiri AM, Hajomar W, Albarrak AM, Al-Tawfiq JA, Zumla AI, Memish ZA. Transmission of MERS-coronavirus in household contacts. N Engl J Med . 2014;371:828–35.
Chest CT Findings in 2019 Novel Coronavirus (2019-nCoV) Infections from Wuhan, China: Key Points for the Radiologist. Radiology **2020**; 200241 [Preprint]. Available from:https://doi.org/10.1148/radiol.2020200241.